Interference in Air to Ground CDMA Cellular Systems

Interference in Air-to-Ground CDMA Cellular Systems

Besma Smida and Vahid Tarokh

Abstract

For air-to-ground cellular systems with no frequency reuse, we provide an analysis of the inter-cell interference under 3D hexagonal cell planning and a line of sight channel model with no shadowing assumptions. Based on this model, we derive approximate bounds for the inter to intra-cell interference ratio for the air-to-ground link. In addition, we provide upper bounds on the interference and the outage probability for the ground-to-air link. Simulation results demonstrate that our approximations are extremely tight.

This paper was presented in part at the CISS 2008 and IEEE ICC 2008 conferences.

I. INTRODUCTION

Air to ground (ATG) communication systems are emerging as an effective way to provide broadband services to the airborne commercial market, because it provides a relatively inexpensive connectivity solution. For ATG systems, as is the case for the terrestrial cellular systems, the main factor limiting the underlying data rates is the existence of interference. This significantly motivates the quantification of interference in these systems. In particular, simple analytic formulas that avoid extensive simulations are very much sought after.

The current air to ground (ATG)/ground to air (GTA) communications spectrum allocation in the United States, only allows for 3G systems that can operate in paired 1.5 MHz forward and 1.5 MHz reverse link bands. A solution is a narrow-band CDMA system that operates in paired 1.25 MHz forward and 1.25 MHz reverse link bands. Examples of such systems are 1xEVDO Rev0 and RevA (EVolution Data-Only Release 0 and Revision A) systems. These systems usually operate with a frequency reuse factor of one (i.e. no frequency reuse) and can provide peak data rates of 3.1 Mbps in the forward and up to 2.4 Mbps in the reverse links. For such CDMA cellular terrestrial systems, forward link interference is studied in a paper by Bender, Black, Grob, Padovani, Sindhushyana, and Viterbi [1] using standard propagation models and extensive simulations for hexagonal cell plan scenario. However, to the best of our knowledge, there are no analytic formulas that can be applied to avoid these extensive simulations. This is not surprising, since the channel path gains for a terrestrial system is a combination of various path loss, long term (shadowing) and short term (multipath) fading components. Path loss by itself can vary from one end user to the other and significantly depends on the environment. Long term fading also depends heavily on the environment. Short term fading can also be Rician or Rayleigh depending on the propagation scenario. These variations make it extremely hard to avoid simulations and obtain a useful formula for the characterization/computation of the interference [2].

When considering ATG/GTA systems, the situation is significantly different. The ATG/GTA channel is accurately modeled by a line-of-sight channel with no shadowing, where path loss obeys a well-known inverse square exponent law as a function of distance from the transmitter[3]. This makes the ATG/GTA systems simpler to analyze than terrestrial systems. Presently, in the literature the interference for CDMA ATG/GTA systems has been commonly studied through the use of extensive simulations [4], [5], [6]. In fact, very accurate closed form approximations for the interference are possible, and this is the topic of the current paper.

The outline of this paper is given next. In Section II, we present our mathematical model of an ATG/GTA communication system. In Section III, we compute approximations on the interference in ATG/GTA systems. In Section IV, we provide simulation results demonstrating that our bounds are very tight for all practical scenarios of interest. Finally, we draw our conclusions in Section V.

II. System and Channel Model

The ATG/GTA channel can be modeled by a line-of-sight channel with no shadowing except for the earth curvature effect. The line-of-sight scenario represents the transmission at the vicinity of the base station and it is characterized by inverse square law path loss [3]. As the distance between the airborne vehicular and the base station is increased, the radio horizon or radio line of sight (RLOS) is approached, and the signal attenuation is highly increased because of the bulge of the earths spherical surface. The extremely large signal attenuation which occurs beyond RLOS is the main difference between an ATG/GTA interference analysis and a conventional terrestrial analysis. We treat this as a step discontinuity in propagation path loss, at RLOS, from the inverse square law to the near-infinite path loss:

$$PL(d[m])[dB] = \begin{cases} 20\log_{10}(d[m]) + C, & \text{if } d < \text{RLOS}, \\ \approx \ \infty, & \text{if } d > \text{RLOS}, \end{cases} \tag{1}$$

where PL is the path loss, C is a constant which accounts for the system losses, and d is the link distance. Since actual attenuations are in fact quite large beyond RLOS, this is a reasonable approximation. The RLOS distance to the 4/3 earth horizon from an airborne vehicle at the altitude z is given by the simple formula (see Figure 1):

$$\text{RLOS}(z) = \sqrt{2R_t z + z^2} \simeq \sqrt{2R_t z}, \tag{2}$$

where $R_t = 4/3 \times 6378.135$ Km is 4/3 times the radius of the earth. The maximum RLOS, named RLOS_{max}, is given by $\text{RLOS}_{max} = \sqrt{2R_tH_{max}}$.

We consider an air-to-ground cellular mobile system, composed of a number of base stations distributed throughout the service area. The proposed system can cover airborne vehicles flying over and near land areas. We analyze both the air-to-ground ATG link, where the information is transmitted from an airborne vehicular to the base station, and the ground-to-air GTA link, where the base station transmits information to an aircraft[1]. The following assumptions are used throughout this paper:

1) We model the 3D cells by cylindrical cells. We first consider the standard hexagonal cell layout and then approximate each hexagon by a co-centered disc of equal area (Note that a hexagon inscribed in a circle of radius R_c is equal in area to a circle of radius $R_s = \sqrt{\frac{3}{\pi}}R_c$) [7]. We will refer to the cells as either the 3D or cylindrical cells in the remainder of the paper.
2) We assume that the airborne vehicles are uniformly distributed in each cylindrical cell with maximum height H_{max}.
3) We assume omnidirectional antennas at both the base station and the airborne vehicular. This assumption makes the computation tractable. We also propose simple tools to extend our results to the case of sectorized antennas at the base station.
4) We assume perfect power control for the ATG link (for both traffic data and pilot) and transmission at maximum for the GTA link.
5) We assume that an airborne terminal is served by the base station with the strongest channel. Since the ATG channel is modeled by Equation (1), all airborne vehicles are connected to the closest base station.

[1]Please note the confusing standardized meaning of downlink and uplink in the context of air-to-ground communication. Therefore, we decided to adopt the ATG/GTA notation in the remainder of the paper

III. ANALYSIS OF INTERFERENCE

A. Air to Ground Link

The analysis derived here can be viewed as an extension of the method in [8] to three dimensional (3D) cellular systems. We first evaluate the contribution of elements of cell Y to the interference at the base station in cell X. We model each interference source as an element of volume $dV = rdrd\theta_i dz$ as shown in Figure 2. By assuming perfect power control, the base station X receives in expectation an element of power dP_Y (from each element dV):

$$dP_Y = \frac{P}{\pi R_s^2 H_{max}} \times |\alpha_i|^2 \times G_i(r, \theta_i, z) \times \frac{\rho^2}{R_i^2} \times U(\text{RLOS}(z) - R_i)\ dV, \tag{3}$$

where P, a constant, is the power received at the base station, α_i is a random variable modeling the multi-path fading, $G_i(r, \theta_i, z)$ is the antenna gain under which the base station X sees the element of volume dV, $\rho = \sqrt{r^2 + z^2}$ is the distance from dV to the closest base station Y, $R_i = \sqrt{D_i^2 + r^2 + z^2 - 2D_i r \cos\theta_i}$ is the distance from the element of volume dV to the desired cell X, and each of the other terms are shown in Figure 2. Note that we adjust the power received by multiplying by $U(\text{RLOS}(z) - R_i)$, the indicator function, which accounts for propagation up to RLOS only [4]:

$$U(x) = \begin{cases} 1 & x \geq 0, \\ 0 & \text{otherwise}. \end{cases} \tag{4}$$

The total average interference contribution of cell Y to cell X is

$$P_Y = \frac{P}{\pi R_s^2 H_{max}} \int_0^{R_s} \int_0^{2\pi} \int_0^{H_{max}} \text{E}[|\alpha_i|^2] G_i(r, \theta_i, z) \frac{\rho^2}{R_i^2} U(\text{RLOS}(z) - R_i) rdrd\theta_i dz. \tag{5}$$

Since the expectation $\text{E}[|\alpha_i|^2] = 1$, hence the fast (multipath) fading do not affect the mean power level. Let $h_{min} \triangleq \frac{D_i^2 + r^2 - 2D_i r \cos\theta_i}{2R_t}$, thus

$$\text{RLOS}(z) - R_i \geq 0 \quad \Longleftrightarrow \quad z \geq h_{min}. \tag{6}$$

After simple manipulations, we have

$$P_Y = \frac{P}{\pi R_s^2 H_{max}} \int_0^{R_s} \int_0^{2\pi} \int_{h_{min}}^{H_{max}} G_i(r, \theta_i, z) \frac{\rho^2}{R_i^2} U(H_{max} - h_{min}) rdrd\theta_i dz. \tag{7}$$

The following Lemma will be useful for further mathematical developments.

Lemma 1: The function $f(z) = \frac{r^2+z^2}{D_i^2+r^2+z^2-2D_i r\cos\theta_i}$ satisfies

$$\frac{r^2}{D_i^2+r^2-2D_i r\cos\theta_i} \leq f(z) \leq \frac{r^2+z^2}{D_i^2+r^2-2D_i r\cos\theta_i},$$

for $r \ll D_i$ and $z \ll \sqrt{D_i^2+r^2-2D_i r\cos\theta_i}$.

Using Lemma 1, P_Y is bounded by

$$\begin{aligned} P_Y &\leq \frac{P}{\pi R_s^2 H_{max}} \int_0^{R_s}\int_0^{2\pi}\int_{h_{min}}^{H_{max}} G_i(r,\theta_i,z)\frac{r^2+z^2}{D_i^2+r^2-2D_i r\cos\theta_i} U(H_{max}-h_{min}) r dr d\theta_i dz, \\ P_Y &\geq \frac{P}{\pi R_s^2 H_{max}} \int_0^{R_s}\int_0^{2\pi}\int_{h_{min}}^{H_{max}} G_i(r,\theta_i,z)\frac{r^2}{D_i^2+r^2-2D_i r\cos\theta_i} U(H_{max}-h_{min}) r dr d\theta_i dz. \end{aligned} \tag{8}$$

As illustrated in Figure 1, we divided all the cells in the service area into three subsections A, B, and C.

- Subset A includes the cells at a distance $D_i \leq \text{RLOS}_{max} - R_s$, the interference contribution of elements in subset A is named I_{ATG_A}.
- Subset B includes the cells at distance $\text{RLOS}_{max} - R_s \leq D_i \leq \text{RLOS}_{max} + R_s$, the interference contribution of elements in subset B is named I_{ATG_B}.
- Subset C includes the rest of the cells (cells in subset C do not interfere with the cell of interest).

This cell division allows us to eliminate the indicator function $U(x)$ and hence makes the analytical evaluation of the interference possible.

1) Subset A: Next we consider any point (r,θ_i,z) in a cell in subset A, then

$$h_{min} = \frac{D_i^2+r^2-2D_i r\cos\theta_i}{2R_t} \leq H_{max}. \tag{9}$$

Using the above equation, the interference contribution of elements in subset A is

$$I_{ATG_A} = \frac{P}{\pi R_s^2 H_{max}} \sum_{i=1}^{N_A} \int_0^{R_s}\int_0^{2\pi}\int_{h_{min}}^{H_{max}} G_i(r,\theta_i,z)\frac{\rho^2}{R_i^2} r dr d\theta_i dz, \tag{10}$$

where N_A is the total number of cells in subset A. In the remainder of section III-A.1, we assume omnidirectional antennas ($G_i(r,\theta_i,z)=1$) at the base station X. This assumption allows us to derive a closed form for the bounds. We substitute the expression of h_{min} in the lower and upper bound expressions in Equation (8) and integrate over z, θ_i and r to arrive at:

$$I^l_{ATG_A} \leq I_{ATG_A} \leq I^u_{ATG_A}. \tag{11}$$

The bounds $I^u_{ATG_A}$ and $I^l_{ATG_A}$ are defined as:

$$I^u_{ATG_A} = \frac{P}{\pi R_s^2 H_{max}} \sum_{i=1}^{N_A} 2\pi \left(\Gamma_i - \frac{H_{max} R_s^2}{2} - \frac{R_s^4}{8R_t} \right) - \frac{2\pi}{24 R_t^3} \left(\Omega_i \right), \tag{12}$$

$$I^l_{ATG_A} = \frac{P}{\pi R_s^2 H_{max}} \sum_{i=1}^{N_A} 2\pi \left(\Upsilon_i - \frac{H_{max} R_s^2}{2} - \frac{R_s^4}{8R_t} \right), \tag{13}$$

where

$$\begin{aligned} \Gamma_i &= \ln \frac{D_i^2}{D_i^2 - R_s^2} \left(\frac{H_{max} D_i^2}{2} + \frac{H_{max}^3}{6} \right), \\ \Omega_i &= D_i^2 R_s^4 + \frac{R_s^6}{6} + \frac{D_i^4 R_s^2}{2}, \\ \Upsilon_i &= \ln \frac{D_i^2}{D_i^2 - R_s^2} \left(\frac{H_{max} D_i^2}{2} \right). \end{aligned} \tag{14}$$

The second term in Equation (12) can be ignored since it is small. This implies that the interference generated by all the airborne vehicles in subset A is approximately upper bounded by:

$$I^u_{ATG_A} \simeq \frac{P}{\pi R_s^2 H_{max}} \sum_{i=1}^{N_A} 2\pi \left(\Gamma_i - \frac{H_{max} R_s^2}{2} - \frac{R_s^4}{8R_t} \right). \tag{15}$$

2) Subset B: Consider any point (r,θ_i,z) in a cell in subset B, the condition $h_{min} \leq H_{max}$ is not necessarily satisfied. Thus, we add another constraint by considering only airborne vehicles having $\cos\theta_i$ above $\frac{2H_{max}R_t - D_i^2 - r^2}{2D_i r}$ as interference sources. For all airborne vehicles at coordinate (r,θ_i,z) only those with phase $\theta_i \in [-\arccos\frac{-2H_{max}R_t + D_i^2 + r^2}{2D_i r}, \arccos\frac{-2H_{max}R_t + D_i^2 + r^2}{2D_i r}]$ and $h_{min} \leq z \leq H_{max}$ must be considered. Hence, the interference to the desired base station X from all the uniformly distributed users in subset B is:

$$I_{ATG_B} = \frac{P}{\pi R_s^2 H_{max}} \sum_{i=1}^{N_B} \int_0^{R_s} \int_{-\alpha}^{\alpha} \int_{h_{min}}^{H_{max}} G_i(r,\theta_i,z) \frac{\rho^2}{R_i^2} r dr d\theta_i dz. \tag{16}$$

where N_B is the total number of cells in subset B and $\alpha = \arccos\left(\frac{-2H_{max}R_t + D_i^2 + r^2}{2D_i r}\right)$. The integral in Equation (16) has an interesting geometric interpretation. To see that we plot an example of a 3D cell in subset B, in Figure 3. We use this geometric interpretation to further approximate Equation (34).

Approximation 1: In any cell in the subset B, only airborne vehicles within the region limited by $\theta_i \in [-\widehat{\alpha}, \widehat{\alpha}]$ are considered as interference sources, where $\widehat{\alpha} = \arccos\left(\frac{-\sqrt{2H_{max}R_t} + D_i}{R_s}\right)$ and $\widehat{\alpha} \in [0, \pi)$ (see Figure 3).

Thus the interference contribution of elements in subsection B is approximated by:

$$I_{ATG_B} \simeq \frac{P}{\pi R_s^2 H_{max}} \sum_{i=1}^{N_B} \int_0^{R_s} \int_{-\widehat{\alpha}}^{\widehat{\alpha}} \int_{h_{min}}^{H_{max}} G_i(r, \theta_i, z) \frac{\rho^2}{R_i^2} r dr d\theta_i dz, \tag{17}$$

By using Lemma 1 and after some mathematical manipulations, I_{ATG_B} can be bounded by a lower and an upper bound as follows:

$$I_{ATG_B}^l \lesssim I_{ATG_B} \lesssim I_{ATG_B}^u, \tag{18}$$

where $I_{ATG_B}^u$ and $I_{ATG_B}^l$ are defined as:

$$\begin{aligned} I_{ATG_B}^u = & \frac{P}{\pi R_s^2 H_{max}} \sum_{i=1}^{N_B} 2\widehat{\beta}\left(\Gamma_i - \frac{H_{max}R_s^2}{2}\right) - 2\widehat{\alpha}\left(\frac{R_s^4}{8R_t}\right) - \frac{2\widehat{\alpha}\Omega_i + \frac{1}{2}\cos(2\widehat{\alpha})\sin(2\widehat{\alpha})D_i^2R_s^4}{24R_t^3} \\ & + \frac{\frac{4}{3}\sin(2\widehat{\alpha})D_i^3R_s^3 + \frac{4}{5}\sin(2\widehat{\alpha})D_iR_s^5}{24R_t^3}, \end{aligned} \tag{19}$$

$$I_{ATG_B}^l = \frac{P}{\pi R_s^2 H_{max}} \sum_{i=1}^{N_B} \max\left\{0, 2\widehat{\alpha}\left(\Upsilon_i - \frac{H_{max}R_s^2}{2}\right) - 2\widehat{\alpha}\left(\frac{R_s^4}{8R_t}\right)\right\}. \tag{20}$$

and $\widehat{\beta} = 2\arctan\left(\frac{D_i+R_s}{D_i-R_s}\tan\frac{\widehat{\alpha}}{2}\right)$. We assumed in the development of Equations (19) and (20) that $\frac{\widehat{\alpha}}{2} \leq \arctan\left(\frac{D_i+r}{D_i-r}\tan\frac{\widehat{\alpha}}{2}\right) \leq \arctan\left(\frac{D_i+Rs}{D_i-R_s}\tan\frac{\widehat{\alpha}}{2}\right)$ and omnidirectional antennas ($G_i(r,\theta_i,z) = 1$) at the base stations. Also, the last two terms in Equation (19) can be ignored since they are small. This gives the approximation:

$$I_{ATG_B}^u \simeq \frac{P}{\pi R_s^2 H_{max}} \sum_{i=1}^{N_B} 2\widehat{\beta}\left(\Gamma_i - \frac{H_{max}R_s^2}{2}\right) - 2\widehat{\alpha}\left(\frac{R_s^4}{8R_t}\right). \tag{21}$$

3) Subset C: All cells in subset C do not interfere with the cell of interest X.

Dividing by P and summing the contributions from all interfering cells, we conclude that the ATG inter-cell interference ratio is approximated by:

$$\begin{aligned} f_{ATG} \triangleq \frac{I_{ATG_A} + I_{ATG_B}}{P} &\lesssim \frac{I^u_{ATG_A} + I^u_{ATG_B}}{P}, \\ f_{ATG} &\gtrsim \frac{I^l_{ATG_A} + I^l_{ATG_B}}{P}. \end{aligned} \tag{22}$$

The resulting values are very good approximations to the ATG inter-cell interference ratio f_{ATG} and yet analytically tractable. Note that the ratio f_{ATG} is also known as the forward-link interference factor f in CDMA systems.

So far we derived approximated interference bounds for omnidirectional antennas, but for the following study case, we consider sectorized antennas at the base station. We aim to illustrate how sectorized antennas can affect the ATG inter-cell interference ratio f_{ATG}. Assuming that airborne vehicles are independently and identically distributed throughout the service area, the total inter-cell interference seen by aircrafts in each sector is approximated by:

$$I^{\mathcal{D}}_{ATG} \approx \frac{I_{ATG_A} + I_{ATG_B}}{\mathcal{D}}. \tag{23}$$

where $\mathcal{D}$ is the directivity of the antenna [9]. In typical cellular, $\mathcal{D}$ ranges between 3 dB to 10 dB. As the antenna beam pattern is made more narrow, $\mathcal{D}$ increases, and the received interference decreases proportionally. Assuming the intra-cell interference is also divided by $\mathcal{D}$, the inter-cell interference ratio $f^{\mathcal{D}}_{ATG}$ is hence unchanged:

$$f^{\mathcal{D}}_{ATG} \approx f_{ATG}. \tag{24}$$

Sectorized antennas at the base station improve the capacity but did not impact the inter-cell interference ratio f_{ATG}.

B. Ground to Air Link

The GTA link differs from the ATG link in that the power control is not employed. Indeed, the base station transmits at maximum power P_T. In a synchronous GTA link, an airborne vehicular experiences interference from surrounding base stations. This interference will degrade the capacity of the air-to-ground systems. To analyze this problem, we model each aircraft as an element of volume located at (r, θ_i, z) in cell Y as illustrated by Figure 2. The power received from each interfering base station X is:

$$P_X = \frac{P_T}{R_i^2} \times |\alpha_i|^2 \times G_i(r, \theta_i, z) \times U(\text{RLOS}(z) - R_i). \tag{25}$$

Note that, similarly to ATG link, we adjust the power received by multiplying by $U(\text{RLOS}(z) - R_i)$ which accounts for propagation up to RLOS only. The average interference contribution of all base stations in the service area, at the airborne vehicle location (r, θ_i, z) in cell Y, is

$$I_{GTA} = \sum_{i=1}^{N} \frac{P_T}{R_i^2} \text{E}[|\alpha_i|^2] G_i(r, \theta_i, z) U(\text{RLOS}(z) - R_i) = \sum_{i=1}^{N} \frac{P_T}{R_i^2} G_i(r, \theta_i, z) U(\text{RLOS}(z) - R_i), \tag{26}$$

where N is the total number of interfering base stations.

1) GTA Interference Analysis: As mentioned before, we consider 3D cells with the standard hexagonal cell layout on the earth's surface. We divide all the cells in the service into different layers. The number of cells and the cell distance for each layer are listed in Table I and illustrated by Figure 4. This cell division allows us to use series summation in conjunction with some geometrical assumptions to derive a compact form of the maximum interference contribution of each layer. The interference I_{GTA} can take the following form

$$\begin{aligned} I_{GTA} &= \sum_{l=1}^{N_l} I_l, \\ &= \sum_{l=1}^{N_l} \sum_{k=1}^{6l} \frac{P_T}{R_k^2} G_k(r, \theta_i, z) U(\text{RLOS}(z) - R_k), \end{aligned} \tag{27}$$

where N_l is the total number of layers, I_l is the interference contribution of layer l and R_k is the distance from the aircraft to the k-th base station in layer l. Using the specific distribution of base stations in the same layer, I_l is derived as

$$I_l = \sum_{k=1}^{6} \frac{P_T}{R_{k1}^2} G_{k1}(r, \theta_i, z) U(\text{RLOS}(z) - R_{k1}) + \sum_{k=1}^{6(l-1)} \frac{P_T}{R_{k2}^2} G_{k2}(r, \theta_i, z) U(\text{RLOS}(z) - R_{k2}), \tag{28}$$

where $R_{k1}^2 = D_{l1}^2 + r^2 + z^2 - 2D_{l1} r \cos(\theta_i + \theta_{k1})$, $D_{l1} = l\sqrt{3}R_s$, $\theta_{k1} = (k-1)\frac{2\pi}{6}$, $R_{k2}^2 = D_{l2}^2 + r^2 + z^2 - 2D_{l2} r \cos(\theta_i + \theta_{k2})$, $D_{l2} = \frac{\sqrt{3+(1+2(l-1))^2}}{2}\sqrt{3}R_s$ and $\theta_{k2} = (k + \mod(k-1, l-1))\frac{2\pi}{6l}$.

The interference contribution of layer l, I_l, satisfies

$$\begin{aligned} I_l &\leq \sum_{k=1}^{6l} \frac{P_T G_k(r,\theta_i,z)}{D_l^2 + r^2 + z^2 - 2D_l r \cos(\theta_i + \theta_k)} U(\text{RLOS}(z) - R_k), \\ &\leq \sum_{k=1}^{6l} \frac{P_T G_k(r,\theta_i,z)}{D_l^2 + r^2 + z^2 - 2D_l r \cos(\theta_i + \theta_k)} U(z - h_{min}), \\ &\leq \left(\sum_{k=1}^{6l} \frac{P_T G_k(r,\theta_i,z)}{D_l^2 + r^2 + z^2 - 2D_l r \cos(\theta_i + \theta_k)}\right) U(z - h_{min}^l), \\ &\leq \left(\sum_{k=1}^{6l} \frac{P_T G_k(r,\theta_i,z)}{D_l^2 + r^2 - 2D_l r \cos(\theta_i + \theta_k)}\right) U(z - h_{min}^l), \end{aligned} \tag{29}$$

where $R_k^2 = D_l^2 + r^2 + z^2 - 2D_l r \cos(\theta_i + \theta_k)$ and $\theta_k = (k-1)\frac{2\pi}{6l}$. In the development above, we first replace the distance D_{l1} and D_{l2} by $D_l = \min\{D_{l1}, D_{l2}\}$. Secondly, using Equation (6), we replace $U(\text{RLOS}(z) - R_k)$ by $U(z - h_{min})$ where $h_{min} = \frac{D_l^2 + r^2 - 2D_l r \cos(\theta_i + \theta_k)}{2R_t}$. Thirdly, we replace h_{min} by $h_{min}^l = \frac{D_l^2 + r^2 - 2D_l r}{2R_t} \leq h_{min}$. This assumption overestimates the interference, because it overestimates the contribution of any base station in layer l to interference by the sum of those of all base stations in layer l. Finally, we remove z^2 from the denominator.

The following Lemma 2 will be useful in the further mathematical developments.

Lemma 2: The sum $\sum_{i=1}^{L} \frac{1}{D^2 + r^2 - 2Dr\cos(\theta + \theta_i)}$ for $\theta_i = (i-1)\frac{2\pi}{L}$ satisfies

$$\sum_{i=1}^{L} \frac{1}{D^2 + r^2 - 2Dr\cos(\theta + \theta_i)} = \frac{1}{D^2 - r^2}\left[\frac{2LD^L(D^L - r^L\cos(L\theta))}{D^{2L} + r^{2L} - 2D^L r^L \cos(L\theta)} - L\right].$$

The proof is given in the Appendix.

The following observation now follows easily from the above Lemma 2.

$$\max_{\theta} \sum_{i=1}^{L} \frac{1}{D^2 + r^2 + z^2 - 2Dr\cos(\theta + \theta_i)} = \frac{L}{D^2 - r^2}\left(\frac{D^L + r^L}{D^L - r^L}\right).$$

Using this observation and assuming omnidirectional antennas ($G_k(r,\theta_i,z) = 1$) at the base stations, I_l is upper bounded by

$$I_l \leq I_l^u, \tag{30}$$

where, with the help equation of (29), I_l^u is defined as

$$I_l^u = P_T \frac{6l}{D_l^2 - r^2} \left(\frac{D_l^{6l} + r^{6l}}{D_l^{6l} - r^{6l}} \right) U(z - h_{min}^l). \tag{31}$$

This result proves that the maximum interference occurs when the airborne vehicular (r, θ_i, z) is located at the axis specified by $\theta_i \in \{\frac{n\pi}{3}, \text{where } n \text{ is integer}\}$, see Figure 4. Thus, the interference contribution of all base stations in the service area can be upper-bounded as follows

$$I_{GTA} \leq I_{GTA}^u = \sum_{l=1}^{N_l} I_l^u. \tag{32}$$

2) Outage Probability: Ignoring background noise, the signal to total interference and noise ratio $SINR$ at the aircraft location (r, θ_i, z) is

$$\text{SINR}(r, \theta_i, z) \approx \frac{\Theta P_T \rho^{-2}}{\sum_{l=1}^{N_l} I_l^u}, \tag{33}$$

where ρ is the distance from the aircraft to the closet base station, Θ is the fraction of the total cell site power devoted to the aircraft (r, θ_i, z). The outage probability is defined as the probability that the SINR of the desired airborne vehicular does not fall below a certain quality of service threshold δ. The outage probability can then be expressed as

$$\Pr(SINR \leq \delta) = \Pr\left(\frac{\rho^2}{P_T} \sum_{l=1}^{N_l} I_l^u \geq \frac{\Theta}{\delta} \right). \tag{34}$$

In order to compute the outage probability, we need to know the distribution of the SINR, which is a random variable. Due to the complexity of the inter-cell interference terms in Equation (26), it is not possible to obtain an exact distribution. Instead, we will provide an upper bound that will enable us to derive the performance of the GTA link. Presently, in the literature the Chernoff upper bound is usually used when a tight bound on the tail probability is required.

The Chernoff upper bound on Equation (34) is

$$\Pr(SINR \leq \delta) \leq \min_{s>0} \ \exp(-s\frac{\Theta}{\delta}) \ \text{E}_{r,z}[\exp(s\frac{\rho^2}{P_T} \sum_{l=1}^{N_l} I_l^u)] \tag{35}$$

A closed form Chernoff bound is not possible to obtain because of the correlation of the interference terms I_l^u. We will hence use the following generalization of the Cauchy-Schwartz inequality

Lemma 3: For all random variables $X_1, \ldots, X_N$

$$\mathrm{E}[X_1 \times \ldots \times X_N]^Q \leq \mathrm{E}[X_1^Q] \times \ldots \times \mathrm{E}[X_N^Q],$$

where Q is the smallest power-2 number greater than N.

Using Lemma 3, we have

$$\Pr(SINR \leq \delta) \leq \min_{s>0} \ \exp(-s\frac{\Theta}{\delta}) \ \prod_{1}^{N_l} \left(\mathrm{E}_{r,z}[\exp(sQ\frac{\rho^2}{P_T} I_l^u)] \right)^{1/Q} \tag{36}$$

where Q is the smallest power-2 number greater than N_l. We replace the expression of h_{min}^l by $H_{min} = \frac{D_l^2+R_s^2-2D_lR_s}{2R_t}$, $\left(\frac{D_l^{6l}+r^{6l}}{D_l^{6l}-r^{6l}}\right)$ by $\left(\frac{D_l^{6l}+R_s^{6l}}{D_l^{6l}-R_s^{6l}}\right)$, and ρ^2 by $r^2 + H_{max}^2$. Then, we integrate over z and r to arrive at

$$\begin{aligned} \mathrm{E}_{r,z}[\exp(sQ\tfrac{\rho^2}{P_T} I_l^u)] \ \ \leq \ \ & \tfrac{H_{min}}{H_{max}} + \left(\tfrac{H_{max}-H_{min}}{R_s^2 H_{max}}\right) \Big[sA(D_l^2 + H_{max}^2)(\mathrm{Ei}(sA\tfrac{D_l^2+H_{max}^2}{D_l^2-R_s^2}) - \mathrm{Ei}(sA\tfrac{D_l^2+H_{max}^2}{D_l^2})) \\ & - (D_l^2 - R_s^2)\exp(sA\tfrac{D_l^2+H_{max}^2}{D_l^2-R_s^2}) + D_l^2 \exp(sA\tfrac{D_l^2+H_{max}^2}{D_l^2}) \Big], \end{aligned} \tag{37}$$

where $A = 6lQ\frac{D_l^{6l}+R_s^{6l}}{D_l^{6l}-R_s^{6l}}$ and $\mathrm{Ei}(x) = -\int_{-x}^{\infty} \frac{\exp(-t)}{t} dt$ is the exponential integral function. By combining Equations (36) and (37), we obtain a closed-form upper bound of the outage probability of GTA system.

The results obtained for the omnidirectional antennas can be extended to the sectorized scenario. We consider *spatial ergodicity* and assume that the airborne vehicles are independently and identically uniformly distributed throughout the service area. We validate the spatial ergodicity assumptions via extensive simulations. We evaluate the interference numerically by taking into account the beam pattern (one sector, three sectors and six sectors). As expected, the maximum inter-cell interference occurs when the airborne vehicles are located at the axis specified by $\theta_i \in \{\frac{n\pi}{3}, \text{where } n \text{ is integer}\}$ and is approximated by:

$$(I^u)_{GTA}^{\mathcal{D}} \approx \frac{I_{GTA}^u}{\mathcal{D}_{all}} \tag{38}$$

where $\mathcal{D}_{all}$ is the directivity of the sum of all sectors in the same base station.

IV. Numerical Results

The ATG inter-cell interference ratios, f_{ATG}, are computed for different cell radii R_s. The inter-cell interference ratios are obtained analytically and via extensive simulations. As mentioned before, we consider 3D cells with standard hexagonal cell layout on the earth's surface. The number of cells and the cell distance for each layer are listed in Table I. In Figures 5, 6 and 7, we present the results for the ATG link with perfect power control and $H_{max} = 18.3$ km. Figures 5 and 6 show that the bounds in Lemma 1 and the Approximation 1 are very tight. The analytical bounds of Equation (22), illustrated in Figure 7, are also very close to the simulations especially for small/moderate cell radius.

In addition, we compute the outage probability of the GTA system for $R_s = 50$, 100, and 200 km. For comparisons purpose, the exact Chernoff bound on the I_{GTA} of Equation (26) is also obtained through simulations. In Figure 8, we present the results with no power control and $H_{max} = 18.3$ km. Upper bound 1 is derived by simulation of the right side of Inequality (35). Upper bound 2 is the analytical upper bound of the outage probability (see Equations (36) and (37)). As can be seen in the figure, the analytical results are close to the exact simulation of the Chernoff bound for operating point of interest ($\sim 1\%$). The analytical upper bounds are roughly 25% (1 dB) higher than the exact numerical values. We also observe that the upper bound of the interference I^u_{GTA} derived from Lemma 2 (illustrated by upper bound 1) is tight especially for small/moderate cell radius R_s. On the other hand, it can be seen that the Inequality given in Lemma 3 is very tight particularly for high R_s (by comparing the upper bound 2 to the upper bound 1).

V. CONCLUSION

In this paper, we provided analytical bounds of inter-cell interference for ground to airborne cellular communication systems assuming the standard 3D hexagonal cell plan and a line-of-sight channel with no shadowing. We also provided simulation results demonstrating that our bounds are very tight for all practical scenarios of interest. These analytical results may be useful to the network designer, allowing an initial back of envelope calculation of the system performance without the need for lengthy and costly computer simulations.

APPENDIX

In this appendix, we prove Lemma 2. The sum $\sum_{i=1}^{L} \frac{1}{D^2+r^2-2Dr\cos(\theta+\theta_i)}$ for $\theta_i = (i-1)\frac{2\pi}{L}$ satisfies

$$\sum_{i=1}^{L} \frac{1}{D^2+r^2-2Dr\cos(\theta+\theta_i)} = \frac{1}{D^2-r^2}\left[2D\left(\sum_{i=1}^{L} \frac{D-r\cos(\theta+\theta_i)}{D^2+r^2-2Dr\cos(\theta+\theta_i)}\right) - L\right] \tag{39}$$

Then, we exploit equation (671) of [10] to have

$$\sum_{i=1}^{L} \frac{D-r\cos(\theta+\theta_i)}{D^2+r^2-2Dr\cos(\theta+\theta_i)} = L\frac{D^{L-1}(D^L-r^L\cos(L\theta))}{D^{2L}+r^{2L}-2D^Lr^L\cos(L\theta)} \tag{40}$$

The result follows by combining Equations (39) and (40).

REFERENCES

[1] P. Bender, P. Black, M. Grob, R. Padovani, N. Sindhushyana, S. Viterbi, ”CDMA/HDR: a bandwidth efficient high speed wireless data service for nomadic users,” *IEEE Communications Magazine*, vol. 38, no. 7, pp. 70-77, July 2000.

[2] K.S. Gilhousen, I.M. Jacobs, R. Padovani, A.J. Viterbi, L.A. Weaver, C.E. Wheatley, ”On the capacity of a cellular CDMA system,” *IEEE Transactions on Vehicular Technology*, vol. 40, no. 2, pp. 303-312, May 1991.

[3] W.C.Y. Lee, ”Sharing spectrum and harmful interference,” *IEEE Vehicular Technology Conference 2000-Spring*, vol. 3, pp. 1778-1781.

[4] D.W. Matolak, “3-D outside cell interference factor for an air-ground CDMA cellular system, ” *IEEE Transactions on Vehicular Technology*, vol. 49, no. 3, pp. 706-710, May 2000.

[5] B.T. Ahmed, M.C. Ramon, L. de Haro Ariet, “On the capacity of air-ground W-CDMA system (downlink analysis),” *IEEE Vehicular Technology Conference 2003-Spring*, vol. 1, pp. 103-106.

[6] B.T. Ahmed, M.C. Ramon, L. de Haro Ariet, “The capacity of air-ground W-CDMA system (uplink analysis),” *IEEE International Symposium on Personal Indoor and Mobile Radio Communications* 2002, vol. 1, pp. 335-338.

[7] J. Wang and L.B. Milstein, “CDMA overlay situations for microcellular mobile communications,” *IEEE Transactions on Communications*, vol. 43, no. 2/3/4, pp. 603-614, Feb-Mar-Apr 1995.

[8] G.R. Cooper and R.W. Nettleton, “A spread-spectrum technique for high-capacity mobile communications,” *IEEE Transactions on Vehicular Technology*, vol. 27, no. 4, pp. 264-275, November 1978.

[9] T.S. Rappaport, *Wireless commmunications: principles & practice*, Prentice Hall PTR, New Jersey, 1999.

[10] L.B.W. Jolley, *Summation of series*, Constable and Compagny Ltd, London, 1925.

Layer	Number of cells	Cell distance D_i
l	6	$D_{l1} = l\sqrt{3}R_c$
	$6(l-1)$	$D_{l2} = \frac{\sqrt{3+(1+2(l-1))^2}}{2}\sqrt{3}R_c$

TABLE I

CDMA INTERFERING CELL DISTANCE.

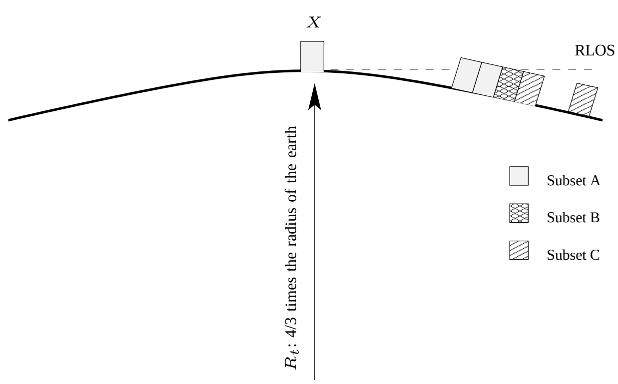

Fig. 1. A cross-section view of the air-to-ground cellular system.

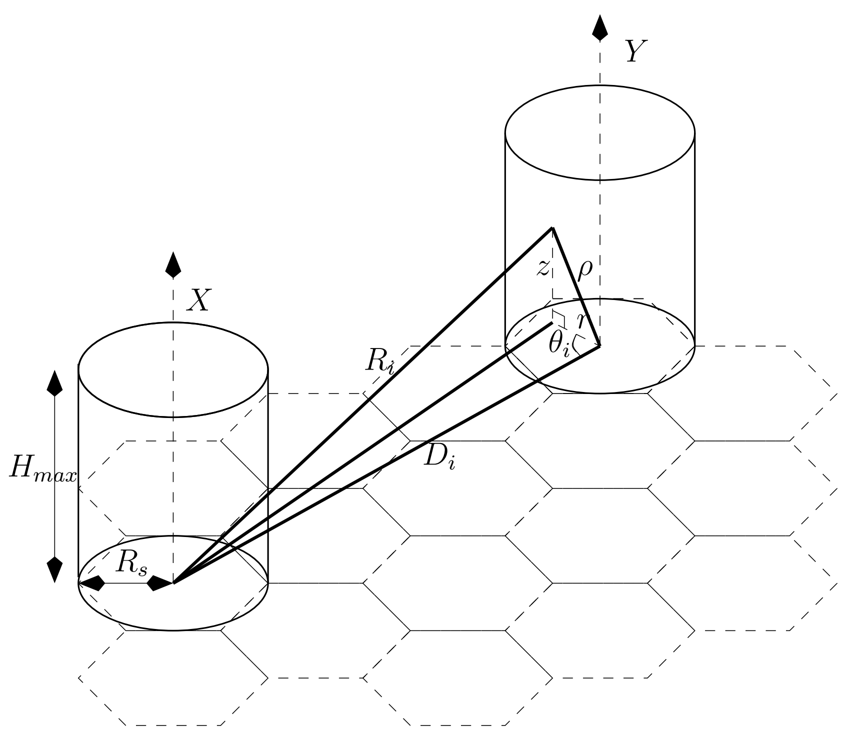

Fig. 2. Illustration of the air-to-ground cellular system (3D view).

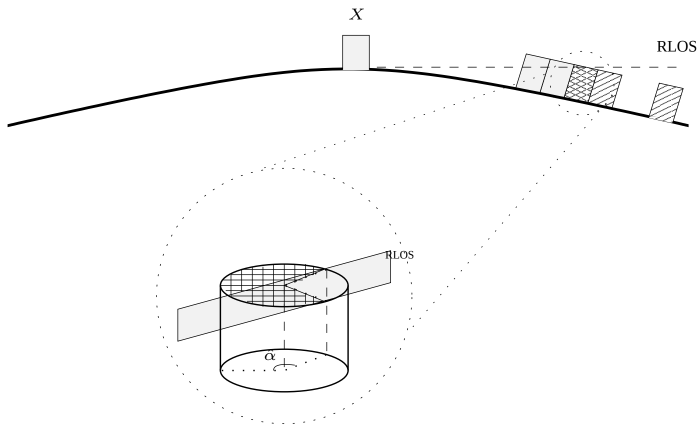

Fig. 3. A 3D cell in subset B.

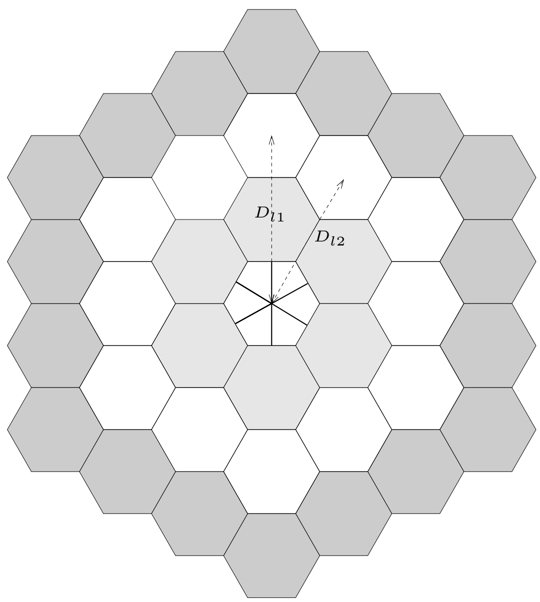

Fig. 4. The hexagonal cell layout on the earth's surface.

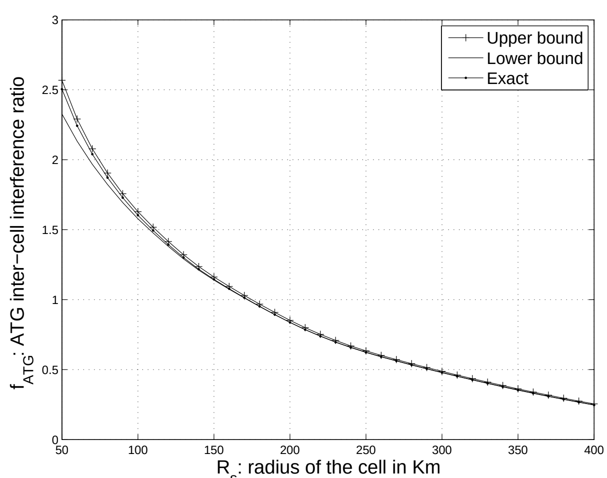

Fig. 5. Analytical and exact (numerical) values of the interference factor f_{ATG} for ATG CDMA cellular (validation of Lemma 1).

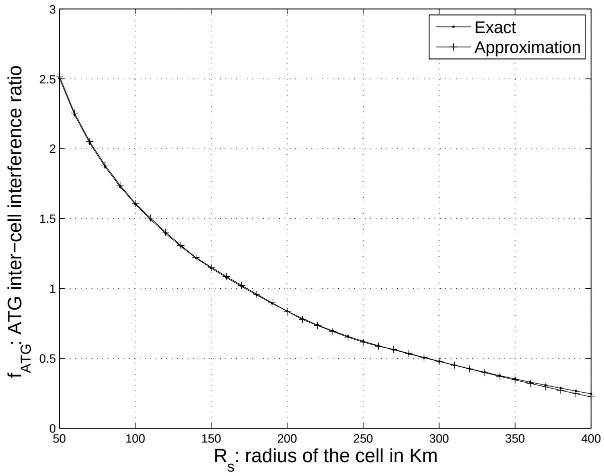

Fig. 6. Analytical and exact (numerical) values of the interference factor f_{ATG} for ATG CDMA cellular (validation of Approximation 1).

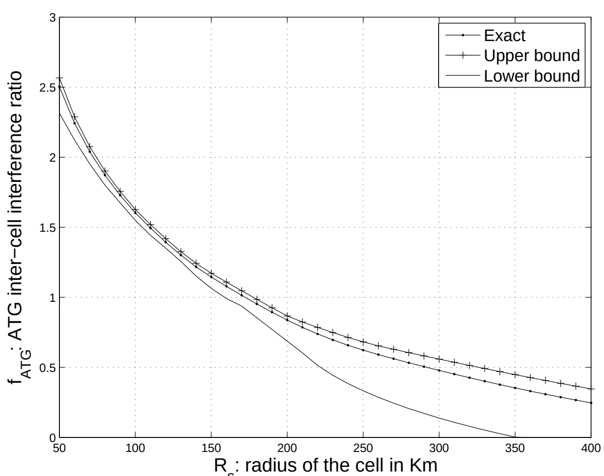

Fig. 7. Analytical and exact (numerical) values of the interference factor f_{ATG} for ATG CDMA cellular (validation of the Equation (22)).

(a)

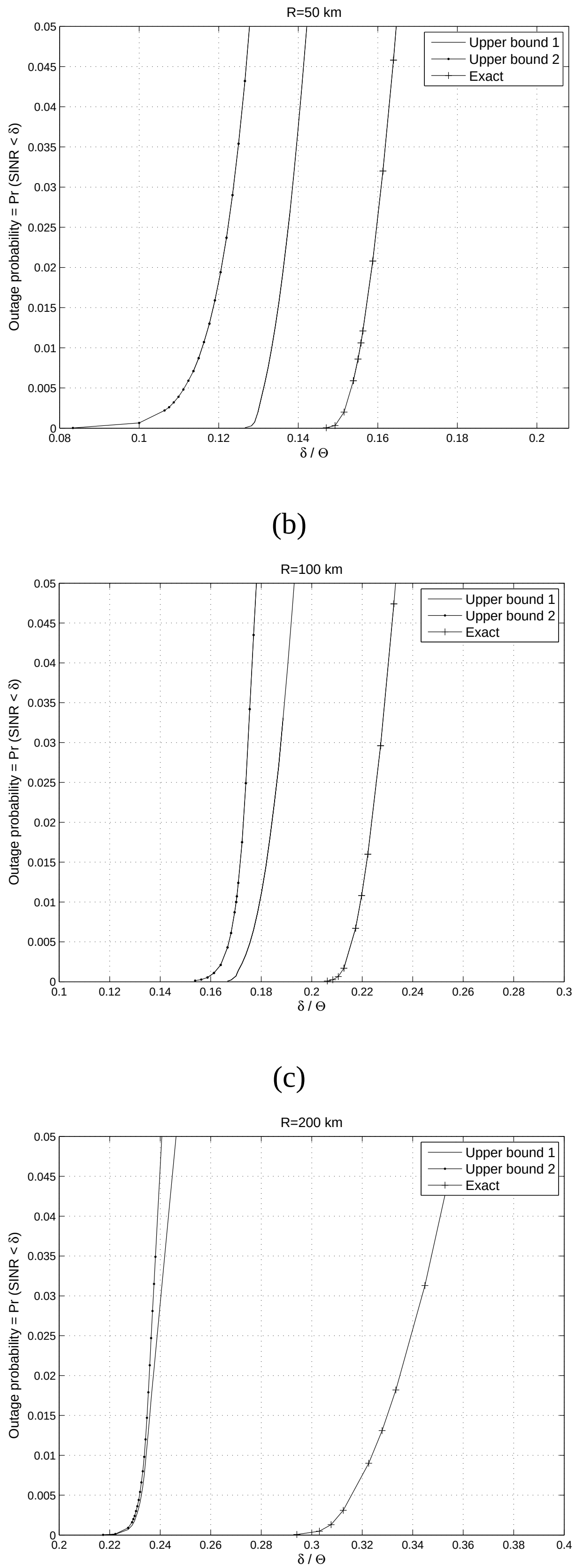

Fig. 8. Analytical and exact (numerical) values of the outage probability of GTA system: (a) $R_s = 50$ km, (b) $R_s = 100$ km and (c) $R_s = 200$ km.